COUPLING EFFECT OF SPLIT RING RESONATOR AND ITS MIRROR IMAGE

F. Zhang[1, *], Q. Zhao[2], J. Sun[3], J. Zhou[3], and D. Lippens[4]

[1]Key Laboratory of Space Applied Physics and Chemistry, Ministry of Education and Department of Applied Physics, School of Science, Northwestern Polytechnical University, Xi'an 710072, P. R. China

[2]State Key Lab of Tribology, Department of Precision Instruments and Mechanology, Tsinghua University, Beijing 100084, P. R. China

[3]State Key Lab of New Ceramics and Fine Processing, Department of Materials Science and Engineering, Tsinghua University, Beijing 100084, P. R. China

[4]Institut d'Électronique de Microélectronique et Nanotechnologies, UMR-CNRS 8520, Université des Sciences et Technologies de Lille, Avenue Poincaré BP 60069, 59652, Villeneuve d'Ascq Cedex, France

Abstract—We report on experimental and numerical studies on the coupling effect of a single split ring resonator (SRR) and its mirror image inside an X-band hollow waveguide. It is shown that, for single SRR with gap bearing side perpendicular to E field, the magnetic resonance exhibits red/blue shift as SRR moves to the gap facing/backing waveguide edge, due to the capacitance and magnetic dipoles coupling effect between original SRR and its mirror image, respectively. Furthermore, electric dipole interplay dominates the coupling effect between SRR and its image when SRR has the gap bearing side parallel to the E field, although SRR is excited by E and H field simultaneously.

1. INTRODUCTION

Electromagnetic metamaterials with unique properties such as negative or zero index have attracted much attention during last decades [1–9]. Exotic research aspects including optics transformation have undergone rapid development with great impact on human's realization

of artificial engineering structure but also brought new force to the advance of novel devices such as invisible cloak [10–22], and Hyperlens [23, 24], perfect absorber [25–29]. Split ring resonator (SRR), the seminal building block of metamaterial, can oscillate with circular currents under proper excitation, subsequently produce a magnetic component opposite to the incident magnetic field, and result in negative permeability around its resonance frequency [30–36]. Such magnetism engineering operations have been demonstrated from microwave up to optical range, around the latter of which most of natural materials possessing relative permeability closes to unity [37]. In addition, by incorporating some active devices into SRR prototype, it is feasible to introduce operation frequency shift, which can be described by equivalent LC circuit resonance condition alteration [38–50]. Similar to the electromagnetic response of natural material response, SRR is generally integrated in dense array, and the coupling effects are of paramount importance by introducing spectral splitting and/or resonant frequency shifts [51–59]. Liu et al. report on the stacked SRRs interaction at optical range influences on the magnetic resonances [52, 53]. The separation and rotation of SRR array influence on planar metamaterial configuration were investigated in term of dipole coupling effect at near infrared regime [54–56]. Besides, several contributions have also addressed the role of tight coupling effect in the propagation direction along with the lateral coupling mechanisms at microwaves [57–59].

Up to now, nearly almost unique phenomena of metamaterial including the negative refraction [1], invisible cloaking [10–12], were observed experimentally in a parallel waveguide system, because waveguide system provides quasi mode distribution but also periodic boundaries, especially the latter of which allows few macroscopic metamaterial elements to exhibit the collective behavior of bulk sample. In contrast to previous reports on coupling effect inside SRR array, we investigate experimentally and numerically on the interaction between a physical SRR and its imaged counterpart mirrored by an electric conductor. To this aim, the transmission spectra of a hollow waveguide loaded by a SRR with its varied location along E field direction were recorded. Concerning asymmetric configuration of SRR due to the presence of splitting gap, two cases with respect to the gap bearing side perpendicular or parallel to the E field were studied experimentally and numerically. The frequency shift as a function of SRR locations is interpreted in term of mutual coupling effect between original SRR and its image counterpart to better understand the underlying physics of frequency change of SRR.
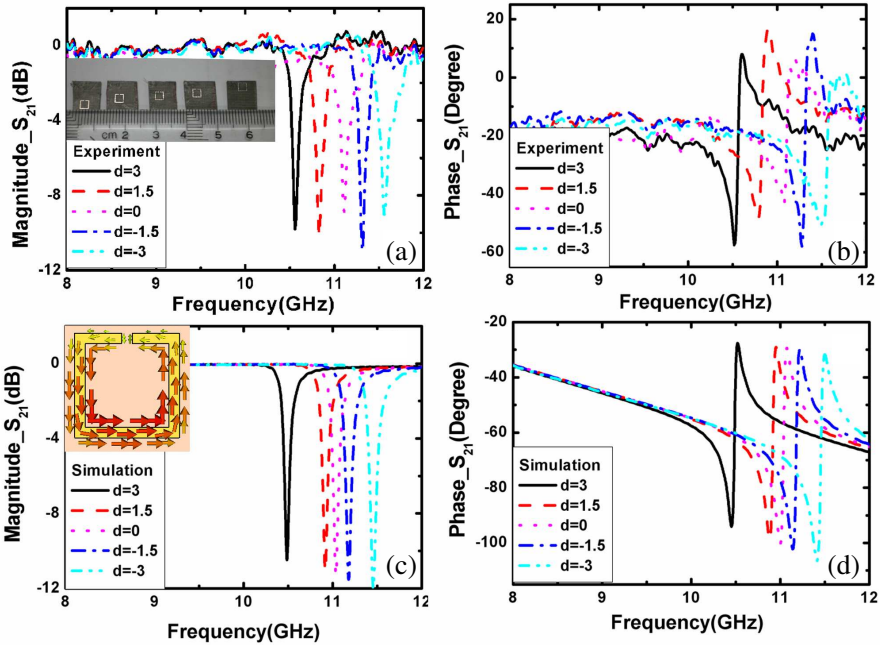
2. EXPERIMENTS AND SIMULATION

2.1. SRR with GAP Bearing Side Perpendicular to E Field

In this manuscript, we employed conventional SRR configuration with single square ring incorporated with one gap, as illustrated in Figure 1. Using commercial printed circuit board technology, the experimental SRR sample was etched on a Teflon fiberglass substrate ($\varepsilon_r = 2.45$, $\tan \delta = 0.003$) with a thickness of 0.8 mm. The SRR substrate were diced with the dimensions of $10.0 \times 5.0\,\mathrm{mm}^2$ so as to match the height of X band waveguide (cross section: $22.86 \times 10.16\,\mathrm{mm}^2$).

For the experimental measurement, SRR sample was then inserted in the middle of an X-band waveguide operating between 8 and 12 GHz as illustrated in Figure 1(a). Due to the asymmetric configuration of SRR, the gap facing and backing surfaces of waveguide are termed as the top and bottom edges, respectively. The SRR location shifts along x axis is labeled by the distance of its center away from the middle line between the top and bottom edges (The dashed line in Figure 1(a)). The shifting distance of SRR center from central line of waveguide, d, is labeled by positive and negative signs when SRR moves towards top and bottom plates, respectively. The transmission spectra of SRR
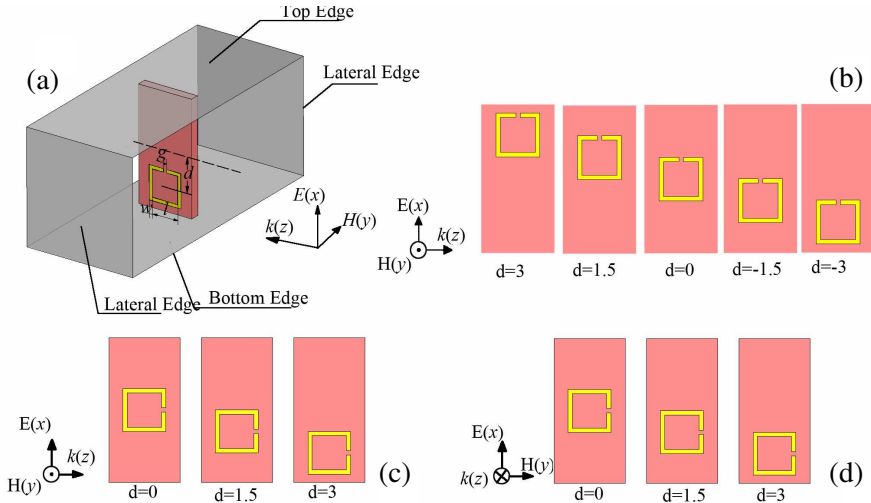
Figure 1. (a) Schematic view for one SRR under grazing incidence via an X band waveguide. The geometrical dimensions for SRR are as follows: $l = 2.4$, $w = g = 0.3$ (unit: mm). Schematic of various SRR samples with gap bearing side (b) perpendicular and (c) parallel to the x axis. (d) SRRs were illuminated under normal incidence.

Figure 2. (a), (b) Experimental and (c), (d) simulated transmission spectra of SRR as a function of its location along E field direction. The insets of (a) and (c) provide the photograph of SRRs with varied locations and induced surface currents of SRR at resonance frequency, respectively.

with various positions were measured and recorded by an HP 8720Es Vector Network Analyzer.

Figure 2 gives transmission spectra of SRR as a function of its positions. For all cases a pronounced dip can be noticed in the spectra which can be anticipated to be a magnetic resonance owing to the axial polarization of the incident H field. When SRR is located exactly in the middle of waveguide ($d = 0$ mm), SRR exhibits a pronounced transmission minimum around 11.0 GHz, which is concomitant with phase jump by nearly $90°$, a symbol indicative of the sign of effective permeability change. As SRR moves towards to the top edge, i.e., with gradually increasing d up to 3.0 mm, the resonance frequency shifts gradually from 11.0 GHz down to 10.56 GHz. On the contrary, resonance frequency monotonically increases up to 11.56 GHz when SRR approaches to the bottom edge. A clear frequency shift of phase jump was also observed in accordance with transmission dip change trend, further confirming the opposite frequency shift for SRR with

respect to the positive or negative value of d. Quantatively, moving SRR position by 6.00 mm from the proximity of bottom edge towards top edge of the waveguide, the resonance frequency varies by more than 1.0 GHz, accounting for nearly 9%.

The simulations were carried out by using a finite time domain package, CST Microwave Studio. SRR was defined by copper with conductivity $\sigma = 5.8 \times 10^7$ S/m. The numerical transmission spectra were calculated rigorously in a hollow waveguide environment and given in Figures 2(c) and (d). The circular surface current monitored around the resonance frequency confirms the magnetic resonance assumption as stated above (See the inset of Figure 2(c)). The simulated transmission spectra point a continuous decrease of the magnetic resonance as the SRR moves from the proximity of bottom edge to top one, showing a quantitative agreement with experimental results. From the application point of view, it is worth mentioning that the fractional change of the resonant frequency around 9% is quite remarkable in comparison with the shift achieved by means of active devices [38–49].

At this stage, one can conclude that a single SRR inserted inside a hollow waveguide is equivalent to one column SRR array, as shown in Figure 3(a), due to a mirror-like effect of the metal walls, which behave as perfect electrical conductors [60]. Obviously, the actual magnetic resonance state of SRR is a net collective response of original single SRR and its image counterparts with reverse gap orientation. For the common case with SRR located in the middle line of the waveguide, magnetic resonance of SRR is the collective resonances between SRR and its imaged cells with gap facing to and backing to each other. When SRR moves towards to the gap facing top edge, i.e., d increases from 0 mm to 3.0 mm, SRR and its imaged counterpart become closer (See Figure 3(b)). Intuitively, it seems that an increasing resonance frequency of SRR can be expected since the transverse magnetic dipole coupling occurs. However, the closer space between SRR and its image as well as top edge of the waveguide enhances the fringing electric field strength around SRR's gap, giving rise to an increase of gap capacitance, hence, a decrease of magnetic resonance because $\omega = \sqrt{LC}$, where L and C present the inductance and capacitance of SRR, respectively. On the other hand, as SRR shifts towards the bottom plates, i.e., d changes from 0 mm to -3 mm, SRR and its imaged counterpart become closer but with a large separation between the two splits, as shown in Figure 3(c)). In this case, only the interactions between magnetic dipoles, formed by oscillation of circular currents of SRR and its imaged counterpart, dominate the resulting resonance frequency. It is therefore the magnetic resonance will shift
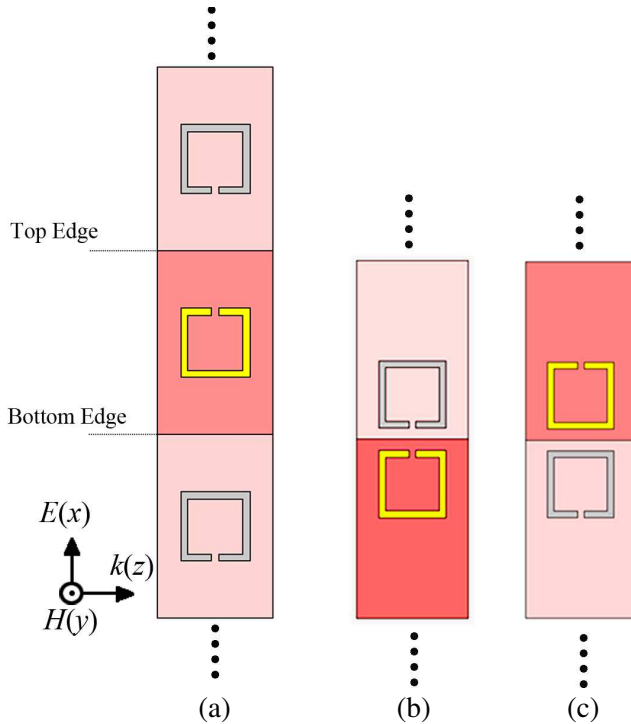
Figure 3. Schematic view of equal periodic array of one SRR located at waveguide, i.e., original SRR located at the central line of waveguide and its imaged periodic counterparts along x directions due to the top and bottom metal boundaries of waveguide. (a) SRR located at the center of waveguide. SRR closes to (b) the top and (c) bottom metal edges of waveguide. The yellow ring represent the original SRR and the gray ones its imaged counterparts.

towards higher frequency as the transverse coupling between magnetic dipole and its image increases.

2.2. SRR with GAP Bearing Side Parallel to E Field under Grazaing Incidence

In this section, we explore the magnetic resonance frequency variation of SRR with its gap bearing side parallel to the incidence E field as shown in Figure 1(c). In this case, SRR are symmetric one with respect to the top and bottom edges of waveguide but asymmetry concerning the incident E field. Compared with SRR of previous configuration, the resonance frequency of SRR rotated by $90°$ with respect to its central
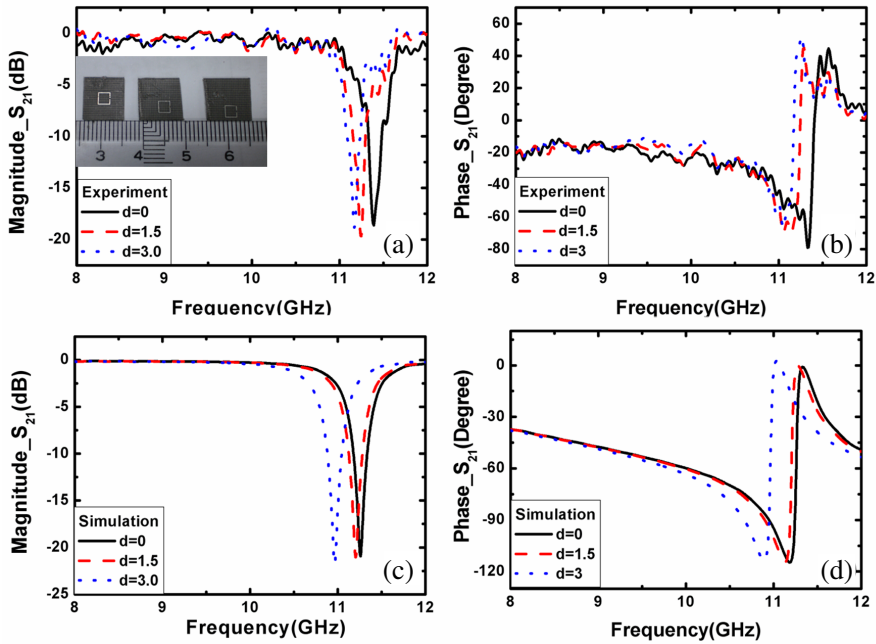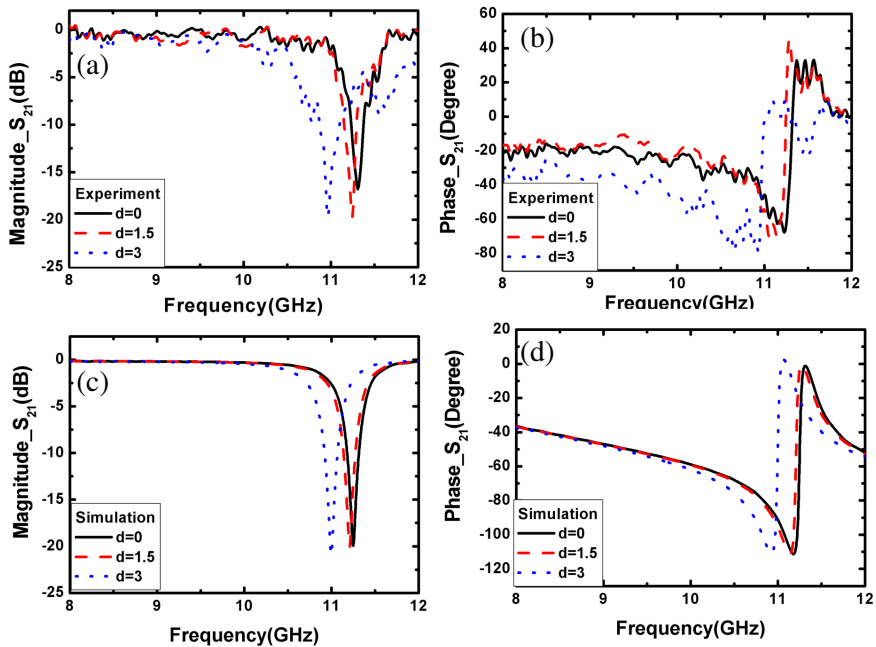
Figure 4. (a), (b) Experimental and (c), (d) simulated transmission spectra of SRR with gap bearing side parallel to x axis and varied as a function of its location along E field direction. The inset displays the photograph of three SRR samples with different locations.

axis, is located at 11.39 GHz (See Figure 4). This is higher than that of previous case, due to the lack of capacitance coupling along E field direction. Furthermore, the transmission dip accounts nearly -20 dB, much stronger than that of the previous case, resulting from an extra circular currents induced by external E field as SRR's asymmetrical configuration with respect the incident electric polarization [61]. As shown in Figure 1(c), when SRR shifts away from the middle line of the waveguide, i.e., d increases from 0 mm to 3.0 mm, the magnetic resonance frequency of SRR is shifted down from 11.39 GHz down to 11.17 GHz. It seems surprising that as much closer between SRR and its image, magnetic resonance is supposed to increase because purely transverse magnetic dipole coupling occurs. Thus, we doubt the emergence of electric dipole induced by the external E field plays effect on the resonance frequency, which will lead to a lower frequency shift because of longitudinal interplays of electric dipole and its image. If so, it means electric dipole induced by the external E field, dominates the coupling effect of SRR magnetic resonance.

2.3. SRR with GAP Bearing Side Perpendicular to E Field under Normal Incidence

To verify our assumption for the electric dipole effect, transmission spectra of SRR with gap bearing side parallel to E field, as shown in Figure 1(d), was measured under normal incidence. Considering there is still a weak H component along z axis in such waveguide setup due to the dominant TE_{10} mode distribution inside waveguide, it is necessary to confirm whether such a magnetic field component can excite SRR resonance. For this purpose, we carried out numerical calculation for SRR with gap bearing side perpendicular to E field under normal incidence, because there is no electric field contribution for SRR and magnetic field component will only the one to excite magnetic resonance if it works. The numerical results shows that no dip can be observed in the given frequency regime, indicating such magnetic field component is too weak (not shown here). Consequently, under normal incidence the sole means to excite the SRR pattern is


Figure 5. (a), (b) Experimental and (c), (d) simulated transmission spectra of SRR under normal incidence. The SRR has a configuration with gap bearing side parallel to x axis and varied location along E field direction.

to orientate the gap arm parallel to the E field direction with thus the possibility to induce circular current by the electromotive force across the gap. It is therefore SRR with gap bearing side parallel to x axis is only excited by E field. As shown from Figure 5, the magnetic resonance of SRR induced by the external E field alone is centered around 11.31 GHz for its location in the middle line of waveguide, which is followed by a lower frequency shift as SRR closes to the metal edge. Obviously, this frequency dependence of SRR on its location along E field direction shows similar tendency of SRR excited by both magnetic and electric field (See Figure 4).

In this case, as the presence of asymmetric configuration of SRR with respect to x axis, circular currents induced by the external E field, giving arise to electric and magnetic dipoles simultaneously. As shown in Figure 6, for the closer interspacing between SRR and its image counterpart, longitudinal coupling between electric dipole and its mirrored image interplay will result in a lower frequency shift as the restoring strength is weaken, whereas the transverse magnetic dipoles coupling contributes to a higher frequency shift [52]. Compared with the experimental and simulated results, we can conclude that electric dipole coupling plays a dominative role in the determination of SRR resonance frequency when SRR excited purely by E field, which is similar to the conclusion point by Refs. [54] and [55]. Importantly, the predominance of electric dipole still exists even magnetic resonance of SRR is excited by external H and E field simultaneously, as mentioned
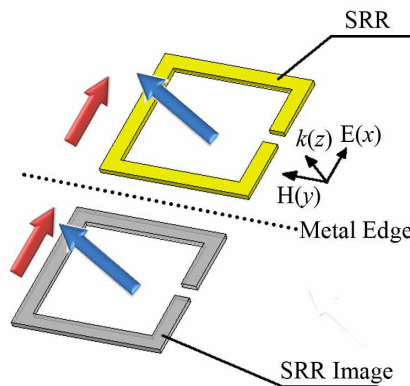
Figure 6. The dipoles distribution of SRR and its imaged counterpart when SRR is illuminated under normal incidence. The blue and red arrows represent the magnetic and electric dipoles, respectively. The original SRR is colored by yellow while the image one by grey.

in Section 2.2. Moreover, this is also further confirmed numerically by two actual SRRs operating under TEM wave illumination in free space (simulation results not shown here).

3. CONCLUSION

In summary, we investigated experimentally and numerically the coupling effect between SRR and its imaged counterpart on the magnetic resonance behavior by changing single SRR location along external E field in an X band waveguide. For SRR with its gap perpendicular to E field, SRR resonance frequency can be tailored red or blue shift as SRR moves to the gap bearing side facing and backing metal edges of waveguide. This can be explained by the capacitive and transverse magnetic dipole coupling between SRR and its imaged counterpart, respectively. For the SRR's gap parallel to E field excited by both the electric and magnetic field, it is shown the magnetic resonance frequency of SRR is lowered when SRR shifts towards metallic plate, as the induced electric dipole coupling between SRR and its imaged counterpart, is stronger than magnetic dipole interplay force. As numerous experimental metamaterial demonstrations were performed in a waveguide system, we believe that the frequency tailored phenomena as well as the underlying coupling mechanism between SRR and its imaged counterpart will enrich the way to tune metamaterial operation frequency and will be useful for the development of metamaterial based devices.

ACKNOWLEDGMENT

REFERENCES

1. Shelby, R. A., D. R. Smith, and S. Schultz, "Experimental verification of a negative index of refraction," *Science*, Vol. 292, 77–79, 2001.
2. Enoch, S., G. Tayeb, P. Sabouroux, and P. Vincont, "A metamaterial for directive emission," *Phys. Rev. Lett.*, Vol. 89, 213902, 2002.

3. Edwards, B., A. Alù, M. E. Young, M. Silveirinha, and N. Engheta, "Experimental verification of epsilon-near-zero metamaterial coupling and energy squeezing using a microwave waveguide," *Phys. Rev. Lett.*, Vol. 100, 033903, 2008.

4. Kang, L., V. Sadaune, and D. Lippens, "Numerical analysis of enhanced transmission through a single subwavelength aperture based on mie resonance single particle," *Progress In Electromagnetics Research*, Vol. 113, 211–226, 2011.

5. Liu, L., J. Sun, X. Fu, J. Zhou, Q. Zhao, B. Fu, J. Liao, and D. Lippens, "Artificial magnetic properties of dielectric metamaterials in terms of effective circuit model," *Progress In Electromagnetics Research*, Vol. 116, 159–170, 2011.

6. Jin, Y. and S. He, "Enhancing and suppressing radiation with some permeability-near-zero structures," *Opt. Express*, Vol. 18, 16587–16593, 2010.

7. Wu, Z., B.-Q. Zeng, and S. Zhong, "A double-layer chiral metamaterial with negative index," *Journal of Electromagnetic Waves and Applications*, Vol. 24, No. 7, 983–992, 2010.

8. Pu, T. L., K. M. Huan, B. Wang, and Y. Yang, "Application of micro-genetic algorithm to the design of matched high gain patch antenna with zero-refractive-index metamaterial lens," *Journal of Electromagnetic Waves and Applications*, Vol. 24, No. 8–9, 1207–1217, 2010.

9. Oraizi, H., A. Abdolali, and N. Vaseghi, "Application of double zero metamaterials as radar absorbing materials for the reduction of radar cross section," *Progress In Electromagnetics Research*, Vol. 101, 323–337, 2010.

10. Schurig, D., J. J. Mock, B. J. Justice, S. A. Cummer, J. B. Pendry, A. F. Starr, and D. R. Smith, "Metamaterial electromagnetic cloak at microwave frequencies," *Science*, Vol. 314, 977–980, 2006.

11. Ma, H. F. and T. J. Cui, "Three-dimensional broadband ground-plane cloak made of metamaterials," *Nature Comm.*, Vol. 1, 21, 2010.

12. Shao, J., H. Zhang, Y. Lin, and H. Xin, "Dual-frequency electromagnetic cloaks enabled by lc-based metamaterial circuits," *Progress In Electromagnetics Research*, Vol. 119, 225–237, 2011.

13. Liu, R., C. Ji, J. J. Mock, J. Y. Chin, T. J. Cui, and D. R. Smith, "Broadband ground-plane cloak," *Science*, Vol. 323, 366–369, 2009.

14. Gaillot, D. P., C. Croënne, and D. Lippens, "An all dielectric route for Terahertz cloaking," *Opt. Express*, Vol. 16, 3986–3992,

2008.

15. Ma, H., S. Qu, Z. Xu, and J. Wang, "Approximation approach of designing practical cloaks with arbitrary shapes," *Opt. Express*, Vol. 16, 15449–15454, 2008.

16. Agarwal, K., X. Chen, L. Hu, H. Liu, and G. Uhlmann, "Polarization-invariant directional cloaking by transformation optics," *Progress In Electromagnetics Research*, Vol. 118, 415–423, 2011.

17. Cheng, X., H. Chen, X.-M. Zhang, B. Zhang, and B.-I. Wu, "Cloaking a perfectly conducting sphere with rotationally uniaxial nihility media in monostatic radar system," *Progress In Electromagnetics Research*, Vol. 100, 285–298, 2010.

18. Valentine, J., J. Li, T. Zentgraf, G. Bartal, and X. Zhang, "An optical cloak made of dielectrics," *Nat. Mater.*, Vol. 8, 568–571, 2009.

19. Chen, X., "Implicit boundary conditions in transformation-optics cloaking for electromagneticwaves," *Progress In Electromagnetics Research*, Vol. 121, 521–534, 2011.

20. Chen, X., Y. Luo, J. Zhang, K. Jiang, J. B. Pendry, and S. Zhang, "Macroscopic invisibility cloaking of visible light," *Nature Comm.*, Vol. 2, 176, 2011.

21. Zhang, B., Y. Luo, X. Liu, and G. Barbastathis, "Macroscopic invisibility cloak for visible light," *Phys. Rev. Lett.*, Vol. 106, 033901, 2011.

22. Chen, H., B.-I. Wu, B. Zhang, and J. A. Kong, "Electromagnetic wave interactions with a metamaterial cloak," *Phys. Rev. Lett.*, Vol. 99, 063903, 2007.

23. Liu, Z., H. Lee, Y. Xiong, C. Sun, and X. Zhang, "Far-field optical hyperlens magnifying sub-diffraction-limited objects," *Science*, Vol. 315, 1686, 2007.

24. Ma, H. F. and T. J. Cui, "Three-dimensional broadband and broad-angle transformation-optics lens," *Nature Comm.*, Vol. 1, 124, 2011.

25. Landy, N. I., S. Sajuyigbe, J. J. Mock, D. R. Smith, and W. J. Padilla, "Perfect metamaterial absorber," *Phys. Rev. Lett.*, Vol. 100, 207402, 2008.

26. Zhu, B., Z. Wang, C. Huang, Y. Feng, J. Zhao, and T. Jiang, "Polarization insensitive metamaterial absorber with wide incident angle," *Progress In Electromagnetics Research*, Vol. 101, 231–239, 2010.

27. Li, M., H.-L. Yang, X.-W. Hou, Y. Tian, and D.-Y. Hou, "Perfect metamaterial absorber with dual bands," *Progress In Electromagnetics Research*, Vol. 108, 37–49, 2010.

28. Huang, L. and H. Chen, "Multi-band and polarization insensitive metamaterial absorber," *Progress In Electromagnetics Research*, Vol. 113, 103–110, 2011.

29. He, X.-J., Y. Wang, J. Wang, T. Gui, and Q. Wu, "Dual-band terahertz metamaterial absorber with polarization insensitivity and wide incident angle," *Progress In Electromagnetics Research*, Vol. 115, 381–397, 2011.

30. Pendry, J. B., A. J. Holden, D. J. Robbins, and W. J. Stewart, "Magnetism from conductors and enhanced nonlinear phenomena," *IEEE Trans. Microw. Theory Tech.*, Vol. 47, 2075–2084, 1999.

31. Marqués, R., F. Mesa, J. Martel, and F. Medina, "Comparative analysis of edge- and broadside-coupled split ring resonators for metamaterial design — Theory and experiments," *IEEE Trans. Antennas Propag.*, Vol. 51, 2572–2581, 2003.

32. Chen, H., L.-X. Ran, B.-I. Wu, J. A. Kong, and T. M. Grzegorczyk, "Crankled S-ring resonator with small electrical size," *Progress In Electromagnetics Research*, Vol. 66, 179–190, 2006.

33. Chen, H., L.-X. Ran, J. T. Huang-Fu, X.-M. Zhang, K.-S. Cheng, T. M. Grzegorczyk, and J. A. Kong, "Magnetic properties of S-shaped split-ring resonators," *Progress In Electromagnetics Research*, Vol. 51, 231–247, 2005.

34. Yao, H.-Y., X. Wei, L.-W. Li, Q. Wu, and T.-S. Yeo, "Propagation property analysis of metamaterial constructed by conductive srrs and wires using the mgs-based algorithm," *IEEE Trans. Microw. Theory Tech.*, Vol. 53, 1469, 2005.

35. Carbonell, J., L. A. Borja, E. V. Boria, and D. Lippens, "Duality and superposition in split-ring-resonator-loaded planar transmission lines," *IEEE Antennas Wireless Propag. Lett.*, Vol. 8, 886–889, 2009.

36. Zhou, L., X. Huang, Y. Zhang, and S.-T. Chui, "Resonance properties of metallic ring systems," *Mater. Today*, Vol. 12, 52–59, 2009.

37. Soukoulis, C. M. and M. Wegener, "Past achievements and future challenges in the development of three-dimensional photonic metamaterials," *Nat. Photon.*, Vol. 5, 523–530, 2011.

38. Gil, I., J. García-García, J. Bonache, F. Martín, M. Sorolla, and R. Marqués, "Varactor-loaded split ring resonators for tunable

notch filters at microwave frequencies," *Electron. Lett.*, Vol. 40, 1347–1348, 2004.

39. NaghshvarianJahromi, M., "Novel compact meta-material tunable quasi elliptic band-pass filter using microstrip to slotline transition," *Journal of Electromagnetic Waves and Applications*, Vol. 24, No. 17–18, 2371–2382, 2010.

40. Park, W.-Y. and S. Lim, "Bandwidth tunable and compact band-pass filter (BPF) using complementary split ring resonators (CSRRs) on substrate integrated waveguide (SIW)," *Journal of Electromagnetic Waves and Applications*, Vol. 24, No. 17–18, 2407–2417, 2010.

41. Chen, H., B.-I. Wu, L. Ran, T. M. Grzegorczyk, and J. A. Kong, "Controllable left-handed metamaterial and its application to a steerable antenna," *Appl. Phys. Lett.*, Vol. 89, 053509, 2006.

42. Feng, T., Y. Li, H. Jiang, W. Li, F. Yang, X. Dong, and H. Chen, "Tunable single-negative metamaterials based on microstrip transmission line with varactor diodes loading," *Progress In Electromagnetics Research*, Vol. 120, 35–50, 2011.

43. Ourir, A., R. Abdeddaim, and J. de Rosny, "Tunable trapped mode in symmetric resonator designed for metamaterials," *Progress In Electromagnetics Research*, Vol. 101, 115–123, 2010.

44. Chen, H.-T., J. F. O'Harai, A. K. Azadi, A. J. Taylor, R. D. Averitt, D. B. Shrekenhamer, and W. J. Padilla, "Experimental demonstration of frequency-agile terahertz metamaterial," *Nat. Photon.*, Vol. 2, 295–298, 2008.

45. Zhang, F., Q. Zhao, L. Kang, D. P. Gaillot, X. Zhao, J. Zhou, and D. Lippens, "Magnetic control of negative permeability metamaterials based on liquid crystals," *Appl. Phys. Lett.*, Vol. 92, 193104, 2008.

46. Lee, S.-W., Y. Kuga, and A. Ishimaru, "Quasi-static analysis of materials with small tunable stacked split ring resonators," *Progress In Electromagnetics Research*, Vol. 51, 219–229, 2005.

47. Khoo, I. C., "Nonlinear optics of liquid crystalline materials," *Phys. Rep.*, Vol. 471, 221–267, 2009.

48. Liu, Q., Y. Cui, D. Gardner, X. Li, S. He, and I. I. Smalyukh, "Self-alignment of plasmonic gold nanorods in reconfigurable anisotropic fluids for tunable bulk metamaterial applications," *Nano. Lett.*, Vol. 10, 1347–1353, 2010.

49. Houzet, G., X. Mélique, D. Lippens, L. Burgnies, G. Velu, and J.-C. Carru, "Microstrip transmission line loaded by split-ring resonators tuned by ferroelectric thin film," *Progress In*

Electromagnetics Research C, Vol. 12, 225–236, 2010.

50. Shen, N., M. Massaouti, M. Gokkavas, J. Manceau, E. Ozbay, M. Kafesaki, T. Koschny, S. Tzortzakis, and C. M. Soukoulis, "Optically implemented broadband blueshift switch in the terahertz regime," *Phys. Rev. Lett.*, Vol. 106, 037403, 2011.

51. Gay-Balmaz, P. and J. F. O. Martin, "Electromagnetic resonances in individual and coupled split-ring resonators," *J. Appl. Phys.*, Vol. 92, 2929–2936, 2002.

52. Liu, N. and H. Giessen, "Coupling effects in optical metamaterials," *Angew. Chem. Int. Ed.*, Vol. 49, 9838–9852, 2008.

53. Liu, N., H. Liu, S. N. Zhu, and H. Giessen, "Stereometamaterials," *Nat. Photon.*, Vol. 3, 157–162, 2009.

54. Feth, N., M. König, M. Husnik, K. Stannigel, J. Niegemann, K. Busch, M. Wegener, and S. Linden, "Electromagnetic interaction of split-ring resonators: The role of separation and relative orientation," *Opt. Express*, Vol. 18, 6545–6554, 2010.

55. Sersic, I., M. Frimmer, E. Verhagen, and A. F. Koenderink, "Electric and magnetic dipole coupling in near-infrared split-ring metamaterial arrays," *Phys. Rev. Lett.*, Vol. 103, 213902, 2010.

56. Decker, M., S. Linden, and M. Wegener, "Coupling effects in low-symmetry planar split-ring resonator arrays," *Opt. Lett.*, Vol. 34, 1579–1581, 2009.

57. Penciu, R. S., K. Aydin, M. Kafesaki, T. Koschny, E. Ozbay, E. N. Economou, and C. M. Soukoulis, "Multi-gap individual and coupled split-ring resonator structures," *Opt. Express*, Vol. 16, 18131–18144, 2008.

58. Carbonell, J., E. Lheurette, and D. Lippens, "From rejection to transmission with stacked arrays of split ring resonators," *Progress In Electromagnetics Research*, Vol. 112, 215–224, 2011.

59. Hesmer, F., E. Tatartschuk, O. Zhuromskyy, A. A. Radkovskaya, M. Shamonin, T. Hao, C. J. Stevens, G. Faulkner, D. J. Edwards, and E. Shamonina, "Coupling mechanisms for split ring resonators: Theory and experiment," *Phys. Stat. Sol.*, Vol. 244, 1170–1175, 2007.

60. Liu, N., H. Guo, L. Fu, S. Kaiser, H. Schweizer, and H. Giessen, "Plasmon hybridization in stacked cut-wire metamaterials," *Adv. Mater.*, Vol. 19, 3628–3632, 2007.

61. Katsarakis, N., T. Koschny, M. Kafesaki, E. N. Economou, and C. M. Soukoulis, "Electric coupling to the magnetic resonance of split ring resonators," *Appl. Phys. Lett.*, Vol. 84, 2943–2945, 2004.